

# Convergence analysis of a hierarchical enrichment of Dirichlet boundary conditions in a mesh-free method

Weimin Han<sup>1,\*</sup>, Gregory J. Wagner<sup>2,†</sup> and Wing Kam Liu<sup>2,§</sup>

<sup>1</sup>*Department of Mathematics, University of Iowa, Iowa City, IA 52242, U.S.A.*

<sup>2</sup>*Department of Mechanical Engineering, Northwestern University, Evanston, IL 60208, U.S.A.*

## SUMMARY

Implementation of Dirichlet boundary conditions in mesh-free methods is problematic. In Wagner and Liu (*International Journal for Numerical Methods in Engineering* 2000; **50**:507), a hierarchical enrichment technique is introduced that allows a simple implementation of the Dirichlet boundary conditions. In this paper, we provide some error analysis for the hierarchical enrichment mesh-free technique. We derive optimal order error estimates for the hierarchical enrichment mesh-free interpolants. For one-dimensional elliptic boundary value problems, we can directly apply the interpolation error estimates to obtain error estimates for the mesh-free solutions. For higher-dimensional problems, derivation of error estimates for the mesh-free solutions depends on the availability of an inverse inequality. Numerical examples in 1D and 2D are included showing the convergence behaviour of mesh-free interpolants and mesh-free solutions when the hierarchical enrichment mesh-free technique is employed. Copyright © 2001 John Wiley & Sons, Ltd.

**KEY WORDS:** mesh-free method; Dirichlet boundary condition; hierarchical enrichment mesh-free technique; error estimate

## 1. INTRODUCTION

Mesh-free methods are a new family of numerical methods that have attracted much attention in the recent years. These new methods have been successfully applied to solve difficult engineering problems involving large deformation, highly localized behaviour such as boundary layers or shear bands, moving discontinuities, etc.

On the other hand, some issues related to the mesh-free methods need further investigation. One of the issues is the implementation of Dirichlet boundary conditions. Unlike the finite

---

\*Correspondence to: Weimin Han, Department of Mathematics, University of Iowa, Iowa City, IA 52242-1419, U.S.A.

†E-mail: whan@math.uiowa.edu

‡E-mail: gjw676@hecky.acns.nwu.edu

§E-mail: w-liu@northwestern.edu

Contract/grant sponsor: NSF

Contract/grant sponsor: ARO

element method, in a mesh-free method, the shape functions do not satisfy the Kronecker delta property at the particles (nodes). This prevents a straightforward application of Dirichlet boundary conditions. Various methods have been proposed in the literature for the treatment of Dirichlet boundary conditions, e.g. the Lagrangian multiplier method [1], coupling with finite elements [2], transformation methods [3], boundary singular kernel method [3], a corrected collocation method in Reference [4], implementation of non-linear boundary condition in Reference [5], etc.

A new method based on a bridging scale is proposed in Reference [6]. This new method offers a simple and efficient way to specify Dirichlet boundary conditions. The bridging scale technique was first introduced in Reference [7]. In this paper, we provide some error analysis for the hierarchical enrichment technique introduced in Reference [6].

We now introduce some notations which we will use in the paper. Let  $\Omega \subset \mathbb{R}^d$  ( $d \geq 1$ ) be a non-empty, open bounded set with a Lipschitz continuous boundary. In the one-dimensional case,  $d=1$ , we choose  $\Omega=(0,L)$  for some  $L>0$ . A generic point in  $\mathbb{R}^d$  is denoted by  $\mathbf{x}=(x_1, \dots, x_d)^T$ , or  $\mathbf{y}=(y_1, \dots, y_d)^T$  or  $\mathbf{z}=(z_1, \dots, z_d)^T$ . We use the Euclidean norm to measure the vector length:

$$\|\mathbf{x}\| = \left( \sum_{i=1}^d |x_i|^2 \right)^{1/2}$$

For  $\mathbf{x}_0 \in \mathbb{R}^d$  and  $r > 0$ , we denote

$$B_r(\mathbf{x}_0) = \{\mathbf{x} \in \mathbb{R}^d: \|\mathbf{x} - \mathbf{x}_0\| \leq r\}$$

for the (closed) ball with radius  $r$  centred at  $\mathbf{x}_0$ . In particular, when  $\mathbf{x}_0 = \mathbf{0}$ , we write  $B_r$  for  $B_r(\mathbf{0})$ .

It will be convenient to use the multi-index notation. Let  $\alpha = (\alpha_1, \dots, \alpha_d)$ ,  $\alpha_i \geq 0$  integer, be a multi-index. The quantity  $|\alpha| = \sum_{i=1}^d \alpha_i$  is the length of  $\alpha$ . We use the notations  $\alpha! = \alpha_1! \cdots \alpha_d!$  and  $\mathbf{x}^\alpha = x_1^{\alpha_1} \cdots x_d^{\alpha_d}$ .

The rest of the paper is organized as follows. In Section 2, we review the hierarchical enrichment technique introduced in Reference [6]. In Section 3, we review the reproducing kernel particle method and its properties. In Section 4, we derive error estimates for the hierarchical enrichment mesh-free interpolants. In Section 5, we present some error estimates for the mesh-free solutions of boundary value problems. The final section is devoted to some numerical examples.

## 2. A HIERARCHICAL ENRICHMENT MESH-FREE APPROXIMATION

To develop a mesh-free approximation, we choose a set of points  $\{\mathbf{x}_I\}_{I \in \mathcal{A}} \subset \bar{\Omega}$ . A point  $\mathbf{x}_I$ ,  $I \in \mathcal{A}$ , is called a particle. The idea of the particle approximation is to use particle function values for approximation:

$$u(\mathbf{x}) \approx \sum_{I \in \mathcal{A}} \Phi_I(\mathbf{x}) u(\mathbf{x}_I) \quad (1)$$

Here  $\{\Phi_I\}_{I \in \mathcal{A}}$  are the shape functions associated with the particles  $\{\mathbf{x}_I\}_{I \in \mathcal{A}}$ . These functions can be constructed by a moving least-squares procedure [8, 1], by a corrected reproducing

kernel particle procedure [9, 10], by *hp*-clouds [11, 12], by partition of unity finite element method [13, 14], or by any other methods. The discussion in this section is valid for any mesh-free shape functions.

Denote the set of the essential boundary nodes by  $\{\mathbf{x}_I\}_{I \in B}$ . We introduce one layer of finite elements on the essential boundary with the nodes  $\{\mathbf{x}_I\}_{I \in B}$ . For each  $I \in B$ , denote  $N_I(\mathbf{x})$  the linear finite element basis function corresponding to the node  $\mathbf{x}_I$ . We have the property  $N_I(\mathbf{x}_J) = \delta_{IJ}$ . Then we introduce the following hierarchical enrichment mesh-free approximations:

$$u^h(\mathbf{x}) = \sum_{I \in B} N_I(\mathbf{x})a_I + \sum_{I \in A} \tilde{\Phi}_I(\mathbf{x})d_I \tag{2}$$

where

$$\tilde{\Phi}_I(\mathbf{x}) = \Phi_I(\mathbf{x}) - \sum_{J \in B} N_J(\mathbf{x})\Phi_I(\mathbf{x}_J) \tag{3}$$

It is easy to verify that for a boundary particle  $\mathbf{x}_I$ ,  $I \in B$ ,  $u^h(\mathbf{x}_I) = a_I$ . Thus, Dirichlet boundary conditions can be specified directly through the coefficients  $\{a_I\}_{I \in B}$ .

It is shown in Reference [6] that from the polynomial reproducing property of the original mesh-free shape functions

$$\sum_{I \in A} \Phi_I(\mathbf{x})\mathbf{x}_I^\alpha = \mathbf{x}^\alpha, \quad \forall \alpha: |\alpha| \leq p$$

we have the consistency of the new mesh-free shape functions:

$$\sum_{I \in B} N_I(\mathbf{x})\mathbf{x}_I^\alpha + \sum_{I \in A} \tilde{\Phi}_I(\mathbf{x})\mathbf{x}_I^\alpha = \mathbf{x}^\alpha, \quad \forall \alpha: |\alpha| \leq p \tag{4}$$

Let us denote by  $\mathcal{P}_p$  the space of the polynomials of degree less than or equal to  $p$ . The dimension of the polynomial space  $\mathcal{P}_p$  is

$$N_p = \binom{p+d}{d} = \frac{(p+d)!}{p!d!}$$

The consistency relations (4) can be equivalently rewritten as

$$\sum_{I \in B} N_I(\mathbf{x})u(\mathbf{x}_I) + \sum_{I \in A} \tilde{\Phi}_I(\mathbf{x})u(\mathbf{x}_I) = u(\mathbf{x}), \quad \forall u \in \mathcal{P}_p \tag{5}$$

### 3. REPRODUCING KERNEL PARTICLE APPROXIMATION

There are various methods to construct mesh-free approximations. In this paper, we focus on the approach of reproducing kernel particle approximation. For this purpose, we first need the so-called *generating function* or *window function*  $\Psi$  with the properties

$$\begin{aligned} &\Psi \text{ is continuous} \\ &\text{supp } \Psi = B_1 \\ &\Psi(\mathbf{x}) > 0 \quad \text{for } \|\mathbf{x}\| < 1 \end{aligned}$$

In one dimension, popular choices in engineering computations include the cubic spline

$$\Psi(z) = \begin{cases} \frac{2}{3} - 4|z|^2 + 4|z|^3, & 0 \leq |z| \leq \frac{1}{2} \\ \frac{4}{3} - 4|z| + 4|z|^2 - \frac{4}{3}|z|^3, & \frac{1}{2} \leq |z| \leq 1 \\ 0, & |z| > 1 \end{cases}$$

and the infinitely smooth function

$$\Psi(z) = \begin{cases} e^{1/(z^2-1)}, & |z| < 1 \\ 0, & |z| \geq 1 \end{cases}$$

Any one-dimensional generating function  $\Psi(z)$  can be used to create a  $d$ -dimensional generating function either in the form  $\Psi(\|z\|)$  or by a tensor product  $\prod_{i=1}^d \Psi(z_i)$ .

We then define

$$\Psi_{r_I}(\mathbf{x} - \mathbf{x}_I) = \Psi\left(\frac{\mathbf{x} - \mathbf{x}_I}{r_I}\right)$$

where the number  $r_I > 0$  is small and represents the support size of the function  $\Psi_{r_I}$ . We use the following form for the shape functions  $\{\Phi_I\}_{I \in A}$ :

$$\Phi_I(\mathbf{x}) = \Psi_{r_I}(\mathbf{x} - \mathbf{x}_I) \sum_{|\alpha| \leq p} (\mathbf{x} - \mathbf{x}_I)^\alpha b_\alpha(\mathbf{x}), \quad I \in A \tag{6}$$

where  $b_\alpha(\mathbf{x})$ ,  $|\alpha| \leq p$ , are the coefficients to be determined by reproducing conditions. Since the domain  $\Omega$  is assumed to be Lipschitz continuous, it is locally on one side of the boundary. In case the particle  $\mathbf{x}_I$  lies on or close to the boundary so that  $B_{r_I}(\mathbf{x}_I) \cap \partial\Omega \neq \emptyset$ , we redefine the function value  $\Psi_{r_I}(\mathbf{x} - \mathbf{x}_I)$  to be zero outside that side of  $\Omega$  on which the particle  $\mathbf{x}_I$  lies. This is implicitly assumed throughout the paper.

Imposing the polynomial reproducing conditions on formula (1),

$$u(\mathbf{x}) = \sum_{I \in A} \Phi_I(\mathbf{x}) u(\mathbf{x}_I) \quad \forall u \in \mathcal{P}_p \tag{7}$$

we have a linear system for the coefficients  $\{b_\alpha(\mathbf{x})\}_{|\alpha| \leq p}$ :

$$\sum_{|\alpha| \leq p} m_{\alpha+\beta}(\mathbf{x}) b_\alpha(\mathbf{x}) = \delta_{|\beta|,0}, \quad |\beta| \leq p \tag{8}$$

where

$$m_\alpha(\mathbf{x}) = \sum_{I \in A} \Psi_{r_I}(\mathbf{x} - \mathbf{x}_I) (\mathbf{x} - \mathbf{x}_I)^\alpha, \quad |\alpha| \leq p \tag{9}$$

are the *discrete moment functions*.

When the method is defined, the shape functions  $\{\Phi_I\}_{I \in A}$  have the following properties:

1. The shape functions have compact supports:  $\text{supp } \Phi_I \subset B_{r_I}(\mathbf{x}_I)$ .
2. The shape functions  $\{\Phi_I\}_{I \in A}$  form a partition of unity.
3. If  $\Psi \in C^k$ , then  $\Phi_I \in C^k$ ,  $I \in A$ .

4. Assume  $\Psi \in C^k$ . Then

$$\sum_{I \in A} D^\alpha \Phi_I(\mathbf{x})(\mathbf{x} - \mathbf{x}_I)^\beta = (-1)^{|\alpha|} \beta! \delta_{\alpha\beta} \quad \forall |\alpha| \leq k, |\beta| \leq p \tag{10}$$

Here  $\delta_{\alpha\beta}$  equals 1 if  $\beta = \alpha$ , and is zero otherwise.

To describe conditions under which the method is defined and works well, we bring in some definitions.

*Definition 3.1.* A point  $\mathbf{x} \in \bar{\Omega}$  is said to be covered by  $m$  shape functions if there are  $m$  indices  $I_1, \dots, I_m$  such that

$$\|\mathbf{x} - \mathbf{x}_{I_j}\| < r_{I_j}, \quad j = 1, \dots, m$$

*Definition 3.2.* A family of particle distributions  $\{\{\mathbf{x}_I\}_{I \in A}\}$  is said to be  $(r, p)$ -regular (or we simply say the particle distributions are  $(r, p)$ -regular) if there is a constant  $L_0$  such that

$$\max_{\mathbf{x} \in \bar{\Omega}} \|M_0(\mathbf{x})^{-1}\|_2 \leq L_0$$

for all the particle distributions in the family. Here  $M_0(\mathbf{x})$  is the *scaled discrete moment matrix*:

$$M_0(\mathbf{x}) = \sum_{I \in A} \Psi\left(\frac{\mathbf{x} - \mathbf{x}_I}{r_I}\right) \mathbf{h}\left(\frac{\mathbf{x} - \mathbf{x}_I}{r}\right) \mathbf{h}\left(\frac{\mathbf{x} - \mathbf{x}_I}{r}\right)^T$$

with

$$\mathbf{h}(\mathbf{z}) = (\mathbf{z}^\alpha)_{|\alpha| \leq p} \in \mathbb{R}^{N_p}$$

Since on a finite-dimensional space all norms are equivalent, the spectral norm  $\|\cdot\|_2$  in the above definition can be replaced by any other matrix norm. We observe that the essential point is to have  $M_0(\mathbf{x})^{-1}$  uniformly bounded, or equivalently, the vectors  $\{\mathbf{h}((\mathbf{x} - \mathbf{x}_I)/r)\}$ , for which  $\Phi((\mathbf{x} - \mathbf{x}_I)/r) \geq c_0 > 0$ , are ‘uniformly’ independent. The particle distribution regularity condition will play an important role in error estimates of mesh-free interpolants and mesh-free solutions. We now mention some examples of regular family of particle distributions; details are found in Reference [15].

*Example 3.3.* The first example is for a one-dimensional domain, that is taken to be  $\Omega = (0, L)$  for some  $L > 0$ . Consider the case of quasiuniform support sizes, i.e. there exist two constants  $c_1, c_2 \in (0, \infty)$  such that

$$c_1 \leq \frac{r_I}{r_J} \leq c_2 \quad \forall I, J \in A$$

For such particle distributions, there exists a parameter  $r > 0$  such that

$$\tilde{c}_1 \leq \frac{r_I}{r} \leq \tilde{c}_2 \quad \forall I \in A$$

Assume there exist two constants  $c_0 > 0, \sigma_0 > 0$  such that for any  $x \in [0, L]$ , there are  $I_0 < I_1 < \dots < I_p$  with

$$\min_{0 \leq j \leq p} \Phi\left(\frac{x - x_{I_j}}{r_{I_j}}\right) \geq c_0 > 0 \tag{11}$$

and

$$\min_{j \neq k} \left| \frac{x_{I_j} - x_{I_k}}{r} \right| \geq \sigma_0 > 0 \tag{12}$$

Then the family of particle distributions  $\{\{x_I\}_{I \in A}\}$  is  $(r, p)$ -regular, i.e. there exists a constant  $L(c_0, \sigma_0)$  such that

$$\max_{0 \leq x \leq L} \|M_0(x)^{-1}\|_2 \leq L(c_0, \sigma_0) \tag{13}$$

Notice that condition (12) can be equivalently written as

$$\min_{0 \leq j \leq p-1} \frac{x_{I_{j+1}} - x_{I_j}}{r} \geq \sigma_0 > 0$$

A geometrical interpretation of condition (12) is that in any local region, at least  $p+1$  particles do not coalesce as the refinement goes to infinity (i.e. as  $r \rightarrow 0$ ).

In the special case of equal support size  $r_I = r$  for any  $I \in A$ , and where  $\Psi$  is increasing on  $[-1, 0]$  and decreasing on  $[0, 1]$  and is symmetric with respect to 0 (always valid in actual computations), if for any  $x$ , we can find  $I_{-1} < I_0 < \dots < I_{p+1}$  such that

$$|x - x_{I_j}| \leq r, \quad -1 \leq j \leq p + 1$$

with

$$\min_{-1 \leq j \leq p} \frac{x_{I_{j+1}} - x_{I_j}}{r} \geq \sigma_0 > 0$$

then (11) is automatically satisfied with

$$c_0 \geq \Psi(1 - \sigma_0)$$

*Example 3.4.* Let  $\Omega \subset \mathbb{R}^d$ . Again consider the case of quasiuniform support sizes. A family of particle distributions  $\{\{\mathbf{x}_I\}_{I \in A}\}$  in  $\mathbb{R}^d$  is  $(r, 1)$ -regular if there exist two constants  $c_0, \tilde{c}_0 > 0$  such that for any  $\mathbf{x} \in \tilde{\Omega}$ , there are  $d + 1$  particles  $\mathbf{x}_{I_0}, \dots, \mathbf{x}_{I_d}$  satisfying

$$\min_{0 \leq j \leq d} \Psi\left(\frac{\mathbf{x} - \mathbf{x}_{I_j}}{r}\right) \geq c_0 > 0$$

and the  $d$ -simplex with the vertices  $\mathbf{x}_{I_0}, \dots, \mathbf{x}_{I_d}$  has a volume larger than  $\tilde{c}_0 r^d$ .

We have the following result for bounds on the shape functions and their derivatives.

*Theorem 3.5.* Assume the particle distributions are  $(r, p)$ -regular and the generating function  $\Psi$  is  $k$ -times continuously differentiable. Then there exists a constant  $c$  such that

$$\max_{I \in A} \max_{\beta: |\beta|=l} \|D^\beta \Phi_I\|_\infty \leq \frac{c}{r^l}, \quad 0 \leq l \leq k$$

#### 4. INTERPOLATION ERROR ESTIMATES

From now on, we assume  $\Psi \in C^1$ . Then we have the regularity property

$$\Phi_I \in C^1(\tilde{\Omega}), \quad I \in A \tag{14}$$

Given a continuous function  $u \in C(\bar{\Omega})$ , we define its hierarchical enrichment mesh-free interpolant to be (cf. (2))

$$u^I(\mathbf{x}) = \sum_{I \in B} u(\mathbf{x}_I) N_I(\mathbf{x}) + \sum_{I \in A} u(\mathbf{x}_I) \tilde{\Phi}_I(\mathbf{x}) \tag{15}$$

We now derive some error estimation for the mesh-free interpolant (15). First, we collect some bounds on the mesh-free shape functions and the linear finite element basis functions. We will always assume that the particle distributions are  $(r, p)$ -regular. From Theorem 3.5, we have

$$\|D^\alpha \Phi_I\|_\infty \leq c r^{-|\alpha|}, \quad \forall \alpha: |\alpha| \leq 1, \quad \forall I \in A \tag{16}$$

We assume the finite elements on the boundary belong to a regular finite element partition of  $\bar{\Omega}$  (cf. References [16, 17]) with the meshsize  $O(r)$ . Then for the finite element basis functions, we have the bounds

$$\int_{\Omega} [|D^\alpha N_I(\mathbf{x})|]^2 dx \leq c r^{1-2|\alpha|} \quad \forall \alpha: |\alpha| \leq 1 \tag{17}$$

Let  $u \in H^{p+1}(\Omega)$ . We assume  $p > d/2 - 1$ . Then by the Sobolev embedding theorem,  $u \in C(\bar{\Omega})$ , and its mesh-free interpolant (15) is well defined. For error analysis, we assume that the family of particle distributions is  $(r, p)$ -regular and the following hypothesis is satisfied.

*Hypothesis (H).* There is a constant integer  $I_0$  such that for any  $\mathbf{x} \in \bar{\Omega}$ , there are at most  $I_0$  of  $\mathbf{x}_I$  satisfying the relation  $\|\mathbf{x} - \mathbf{x}_I\| < r_I$ , i.e. each point in  $\bar{\Omega}$  is covered by at most  $I_0$  shape functions.

Hypothesis (H) is quite natural since otherwise as the number of shape functions covering a local area increases, the shape functions tend to be more and more linearly dependent on the local area.

We will apply results concerning polynomial approximations of Sobolev functions found in Reference [16, chapter 4]. For this purpose, we first introduce some concepts. Let  $B$  be a ball. Then a domain  $\Omega_0$  is said to be star shaped with respect to  $B$  if for any  $\mathbf{x} \in \Omega_0$ , the closed convex hull of  $\{\mathbf{x}\} \cup B$  is a subset of  $\Omega_0$ . The *chunkiness parameter* of  $\Omega_0$  is defined to be  $\text{diam}(\Omega_0)/\rho_{\max}$ , where

$$\rho_{\max} = \sup\{\rho: \Omega_0 \text{ is star shaped with respect to a ball of radius } \rho\}$$

To simplify the notation, we write  $B_I \equiv B_{r_I}(\mathbf{x}_I)$ ,  $I \in A$ . We first bound the error  $u - u^I$  in Sobolev norms over  $B_J \cap \bar{\Omega}$  for  $J \in A$ . Define

$$\Omega_J = \left\{ \mathbf{x}: \|\mathbf{x} - \mathbf{x}_J\| < r_J + \max_{I \in A} r_I \right\}$$

and let

$$A_J = \{I \in A: \text{dist}(\mathbf{x}_I, B_J) < r_I\}$$

Then by hypothesis (H), the number of elements in the sets  $A_J$ ,  $J \in A$ , is uniformly bounded. If  $\bar{\Omega}_J \subset \bar{\Omega}$ , then  $\bar{\Omega}_J \cap \bar{\Omega} = \bar{\Omega}_J$  is star shaped with respect to  $\tilde{B}_J \equiv B_J$ . Now suppose  $\bar{\Omega}_J \not\subset \bar{\Omega}$ .

Then since  $\partial\Omega$  is Lipschitz continuous, if  $r$  is sufficiently small, we can choose a ball  $\tilde{B}_J$  of radius  $r_J/2$  with  $\mathbf{x}_J$  on its boundary such that  $\tilde{\Omega}_J \cap \tilde{\Omega}$  is star shaped with respect to  $\tilde{B}_J$ . We observe that the chunkiness parameters of  $\tilde{\Omega}_J \cap \tilde{\Omega}$ ,  $J \in A$ , are uniformly bounded.

Let  $Q_J^p u$  be the Taylor polynomial of degree  $p$  of  $u$  averaged over  $\tilde{B}_J$ ; the definition and properties of  $Q_J^p u$  can be found in Reference [16, Section 4.1]. Denote the error

$$R_J^p u(\mathbf{x}) = u(\mathbf{x}) - Q_J^p u(\mathbf{x})$$

Then, since the chunkiness parameters of  $\tilde{\Omega}_J \cap \tilde{\Omega}$  are uniformly bounded when  $r$  is sufficiently small, from the results of Reference [16, Section 4.3], we have the estimates:

$$\|R_J^p u\|_{L^2(\Omega_J \cap \Omega)} \leq cr^{p+1} |u|_{H^{p+1}(\Omega_J \cap \Omega)} \tag{18}$$

$$\|R_J^p u\|_{H^1(\Omega_J \cap \Omega)} \leq cr^p |u|_{H^{p+1}(\Omega_J \cap \Omega)} \tag{19}$$

$$\|R_J^p u\|_{L^\infty(\Omega_J \cap \Omega)} \leq cr^{p+1-d/2} |u|_{H^{p+1}(\Omega_J \cap \Omega)} \tag{20}$$

where the constant  $c$  is independent of  $J$ .

Now for  $\mathbf{x} \in B_J \cap \tilde{\Omega}$ , we write

$$\begin{aligned} u(\mathbf{x}) - u^I(\mathbf{x}) &= Q_J^p u(\mathbf{x}) - \sum_{I \in B} Q_J^p u(\mathbf{x}_I) N_I(\mathbf{x}) - \sum_{I \in A} Q_J^p u(\mathbf{x}_I) \tilde{\Phi}_I(\mathbf{x}) \\ &\quad + R_J^p u(\mathbf{x}) - \sum_{I \in B} R_J^p u(\mathbf{x}_I) N_I(\mathbf{x}) - \sum_{I \in A} R_J^p u(\mathbf{x}_I) \tilde{\Phi}_I(\mathbf{x}) \end{aligned}$$

By the polynomial reproducing property (5),

$$\sum_{I \in B} Q_J^p u(\mathbf{x}_I) N_I(\mathbf{x}) + \sum_{I \in A} Q_J^p u(\mathbf{x}_I) \tilde{\Phi}_I(\mathbf{x}) = Q_J^p u(\mathbf{x})$$

Thus

$$u(\mathbf{x}) - u^I(\mathbf{x}) = R_J^p u(\mathbf{x}) - \sum_{I \in B} R_J^p u(\mathbf{x}_I) N_I(\mathbf{x}) - \sum_{I \in A} R_J^p u(\mathbf{x}_I) \tilde{\Phi}_I(\mathbf{x})$$

Note that  $\mathbf{x}_I \in \tilde{\Omega}_J \cap \tilde{\Omega}$  for  $I \in A_J$ . So using bound (16), we have

$$\begin{aligned} \|u - u^I\|_{H^1(B_J \cap \Omega)} &\leq \|R_J^p u\|_{H^1(B_J \cap \Omega)} + c \|R_J^p u\|_{L^\infty(\Omega_J \cap \Omega)} \\ &\quad \times \left( \sum_{I \in B \cap S_J} \|N_I\|_{H^1(B_J \cap \Omega)} + \sum_{I \in A_J} \|\tilde{\Phi}_I\|_{H^1(B_J \cap \Omega)} \right) \end{aligned}$$

Recall that the number of elements contained in  $A_J$  is uniformly bounded. Applying estimates (19), (20) and (16), we obtain

$$\|u - u^I\|_{H^1(B_J \cap \Omega)} \leq cr^p |u|_{H^{p+1}(\Omega_J \cap \Omega)}, \quad J \in A$$



Hence, by using hypothesis (H) once more, we get the error estimate

$$\|u - u^I\|_{H^1(\Omega)} \leq cr^p |u|_{H^{p+1}(\Omega)} \tag{21}$$

Similarly,

$$\|u - u^I\|_{L^2(\Omega)} \leq cr^{p+1} |u|_{H^{p+1}(\Omega)} \tag{22}$$

Therefore, we have the following result.

*Theorem 4.1.* Assume the particle distributions are  $(r, p)$ -regular,  $p \geq d/2 - 1$ ,  $\Psi \in C^1$ , the finite elements on the boundary are such that (17) holds, and hypothesis (H) is valid. Let  $u \in H^{p+1}(\Omega)$ . Then we have the optimal order interpolation error estimates (21) and (22).

### 5. ERROR ESTIMATES FOR MESH-FREE SOLUTIONS

To explain the mesh-free method and error estimates in a concrete problem setting, we take a linear second-order elliptic boundary value problem as an example.

Let  $\Gamma \subset \partial\Omega$  be a non-trivial closed subset of the boundary  $\partial\Omega$ , and  $g \in H^1(\Omega)$  that is continuous in a neighbourhood of  $\Gamma$ . Consider a second-order elliptic boundary value problem: Find  $u \in H^1(\Omega)$  such that  $u = g$  on  $\Gamma$  and

$$a(u, v) = l(v) \quad \forall v \in V \tag{23}$$

Here

$$V = \{v \in H^1(\Omega) : v = 0 \text{ on } \Gamma\}$$

Assume  $a(\cdot, \cdot)$  is a continuous, coercive bilinear form on  $V$  and  $l$  is a continuous linear form on  $V$ . Then by Lax–Milgram lemma, problem (23) has a unique solution.

On  $\bar{\Omega}$ , introduce a set of particles  $\{\mathbf{x}_I\}_{I \in A}$  and its subset  $\{\mathbf{x}_I\}_{I \in B} \subset \Gamma$ . Also, introduce positive numbers  $\{r_I\}_{I \in A}$ , and construct functions  $\{\Phi_I\}_{I \in A}$  in the form of (6) where  $\{b_x(\mathbf{x})\}_{|x| \leq p}$  are computed from (8). The reproducing kernel particle space is

$$V^h = \text{span}\{\tilde{\Phi}_I, I \in A\}$$

To approximate the boundary condition, let

$$V_\Gamma^h = \text{span}\{N_I, I \in B\}$$

Note that functions in  $V^h$  vanish at the boundary nodes on  $\Gamma$ . We formulate the mesh-free method for (23) as: Find  $u^h \in V^h + V_\Gamma^h$  such that  $u^h = g$  at the boundary nodes on  $\Gamma$  and

$$a(u^h, v^h) = l(v^h) \quad \forall v^h \in V^h \tag{24}$$

As long as  $a(\cdot, \cdot)$  is coercive on  $V^h$ , the discrete problem (24) also admits a unique solution.

In general, the mesh-free method (24) is an external approximation of problem (23), since  $V^h \not\subset V$  and even when  $g = 0$ ,  $u^h \notin V$ . In the one-dimensional case, however, the approximation is conforming as it is easily seen that  $V^h \subset V$ . So we first consider the mesh-free method for a one-dimensional second-order elliptic boundary value problem. Without loss of generality,

let  $\Omega = (0, 1)$  and assume the Dirichlet boundary condition:  $u(0) = g_0$ ,  $u(1) = g_1$ . Let  $N_0$  and  $N_1$  be the corresponding linear finite element basis functions at the nodes  $x_0 = 0$  and  $x_N = 1$ . Then

$$u^h(x) = g_0 N_0(x) + g_1 N_1(x) + \sum_I \tilde{\Phi}_I(x) d_I$$

where

$$\tilde{\Phi}_I(x) = \Phi_I(x) - \Phi_I(0)N_0(x) - \Phi_I(1)N_1(x)$$

We write

$$u^h = w^h + g_0 N_0 + g_1 N_1$$

Then  $w^h \in V^h$  satisfies

$$a(w^h, v^h) = l(v^h) - a(g_0 N_0 + g_1 N_1, v^h) \quad \forall v^h \in V^h$$

This problem has a unique solution. For an error estimation, we can apply Cea's inequality and write

$$\begin{aligned} \|u - u^h\|_{H^1(\Omega)} &= \|w - w^h\|_{H^1(\Omega)} \\ &\leq c \inf_{v^h \in V^h} \|w - v^h\|_{H^1(\Omega)} \\ &\leq c \|w - w^I\|_{H^1(\Omega)} \\ &= c \|u - u^I\|_{H^1(\Omega)} \end{aligned}$$

Assume the  $(r, p)$ -regularity and hypothesis (H). Then if  $u \in H^{p+1}(\Omega)$ , we have the error estimate by using (21):

$$\|u - u^h\|_{H^1(\Omega)} \leq cr^p |u|_{H^{p+1}(\Omega)} \quad (25)$$

Employing the standard duality technique in the theory of the finite element method (cf. References [16, 17]), we then have the error estimate in the  $L^2$  norm:

$$\|u - u^h\|_{L^2(\Omega)} \leq cr^{p+1} |u|_{H^{p+1}(\Omega)} \quad (26)$$

In the general case  $d \geq 2$ , it is much more difficult to obtain error estimates for mesh-free solutions when the Dirichlet boundary conditions are present, due to the fact that  $V^h \not\subseteq V$ . Let  $g = 0$ . Applying the framework on page 196 of Reference [16], we have

$$\|u - u^h\|_{H^1(\Omega)} \leq c \inf_{v^h \in V^h} \|u - v^h\|_{H^1(\Omega)} + c \sup_{v^h \in V^h} \frac{|a(u, v^h) - l(v^h)|}{\|v^h\|_{H^1(\Omega)}} \quad (27)$$

An estimate for the first term on the right-hand side of (27) is derived by applying the interpolation error estimate (21). If an *inverse inequality* of the type

$$\|v^h\|_{H^2(T)} \leq cr^{-1} \|v^h\|_{H^1(T)} \quad \text{for any finite element } T \text{ on } \Gamma, \quad \forall v^h \in V^h \quad (28)$$

holds, then it can be shown that the second term on the right-hand side of (27) is bounded by  $O(r)$ . We will look into the possibility of proving the inverse inequality (28) in the future. Note that in general, the convergence order of method (24) is expected to be one only. To increase the convergence order, one needs to make modifications; one such modification is to include a boundary integral term in the weak formulation (cf. Reference [6]).

6. NUMERICAL RESULTS FOR MESH-FREE INTERPOLANTS WITH A FINITE ELEMENT BOUNDARY

6.1. 1D results: solution and interpolation convergence

An example problem demonstrates the interpolation error estimates (21) and (22) and the solution error estimates (25) and (26) in 1D. Consider the following second-order boundary value problem:

$$a_0 u_{,x} - v u_{,xx} = \sin \frac{\pi x}{L}, \quad 0 \leq x \leq L \tag{29a}$$

$$u(0) = 0 \tag{29b}$$

$$u(L) = 1 \tag{29c}$$

The exact solution is given by

$$u(x) = \frac{1}{\pi(a_0^2 L^2 + \pi^2 v^2)} \left( -L^3 a_0 \cos \frac{\pi x}{L} + L^2 v \pi \sin \pi x L - \frac{-L^3 a_0 e^{ax/L} + e^{a_0 x/v} (2L^3 a_0 - L^2 a_0^2 \pi - \pi^3 v^2) + a_0^2 \pi L^2 + \pi^3 v^2 - L^3 a_0}{e^{a_0 L/v} - 1} \right) \tag{30}$$

The weak formulation of the boundary value problem is to find  $u \in H^1(0, L)$  such that  $u(0) = 0$ ,  $u(L) = 1$ , and

$$a(u, v) = \int_0^L \sin \frac{\pi x}{L} v(x) dx \quad \forall v \in H_0^1(0, L)$$

where the associated bilinear form is

$$a(u, v) = \int_0^L (a_0 u_{,x} v + v u_{,x} v_{,x}) dx$$

Observe that the bilinear form is coercive on the space  $H_0^1(0, L)$  since

$$a(v, v) = v \int_0^L v_{,x}^2 dx \quad \forall v \in H_0^1(0, L)$$

Therefore, our error estimates apply to the mesh-free solution of the boundary value problem.

The problem is solved numerically on a set of nodes with nodal spacing  $h$ . The mesh-free shape functions are the reproducing kernel particle functions described in Section 3; a support size of  $r = 2.2h$  is used for all solutions, and the order of the reproduced polynomial space is  $p$ . Results are presented for the case  $a_0 = 5$ ,  $v = 1$ , and  $L = 1$ . Numerical integration is performed using the Gaussian quadrature with four points between each set of adjacent nodes. The interpolation error is defined as (cf. (15)):

$$u(x) - u^I(x) = u(x) - \sum_{I \in B} N_I(x) u(x_I) - \sum_{I \in A} \tilde{\Phi}_I(x) u(x_I) \tag{31}$$

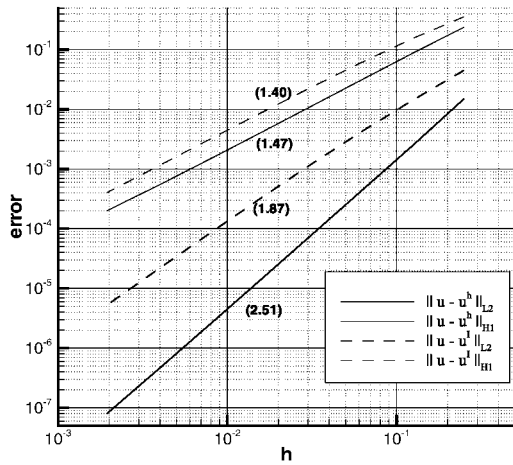


Figure 1. Error vs nodal spacing for 1D RKPM with boundary enrichment: results for  $p=1$ . Convergence rates are shown in parentheses.

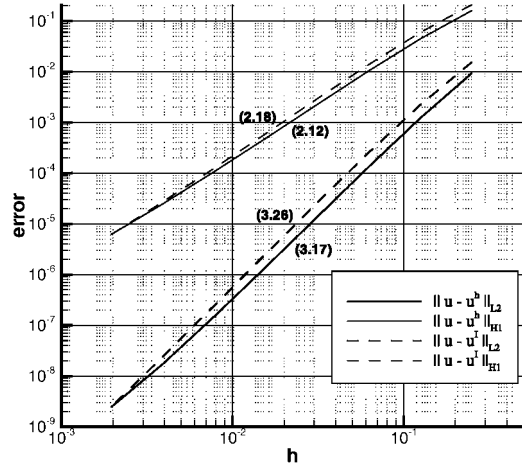


Figure 2. Error vs nodal spacing for 1D RKPM with boundary enrichment: results for  $p=2$ . Convergence rates are shown in parentheses.

The  $L2$  and  $H1$  convergence results for  $p=1$  are shown in Figure 1, while those for  $p=2$  are given in Figure 2. The convergence of both interpolation and solution errors is as predicted in Equations (21), (22), (25) and (26), i.e. order  $p+1$  for  $L2$  and order  $p$  for  $H1$ . Convergence rates given in Figures 1 and 2 are computed by fitting a line through all data points; in several cases (notably the  $L2$  interpolation error for  $p=1$ ), rates asymptote to higher values as  $h \rightarrow 0$ .

6.2. 2D results: solution and interpolation convergence

The solution of a 2D Laplace equation demonstrates the interpolation and solution error estimates in multiple dimensions. The boundary value problem to be solved is

$$\nabla^2 u(x, y) = 0, \quad 0 \leq x \leq 1, \quad 0 \leq y \leq 1 \tag{32a}$$

$$u(x, y) = \sin(\pi x), \quad \text{for } y = 0 \tag{32b}$$

$$u(x, y) = 0, \quad \text{for } x = 0, x = 1 \text{ or } y = 1 \tag{32c}$$

The exact solution, easily obtained through separation of variables, is

$$u(x, y) = [\cosh(\pi y) - \coth \pi \sinh(\pi y)] \sin(\pi x) \tag{33}$$

The Galerkin weak form of (32) is

$$\int_{\Omega} \nabla v \cdot \nabla u \, d\Omega = 0 \tag{34}$$

where  $\Omega$  is the solution domain.

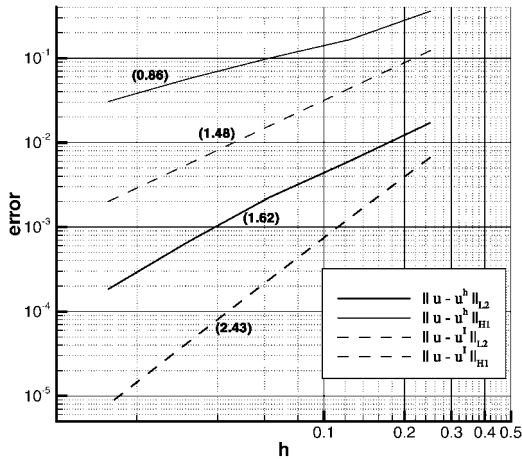


Figure 3. Error vs nodal spacing for 2D RKPM with boundary enrichment: results for  $p=1$ . Convergences rates are shown in parentheses.

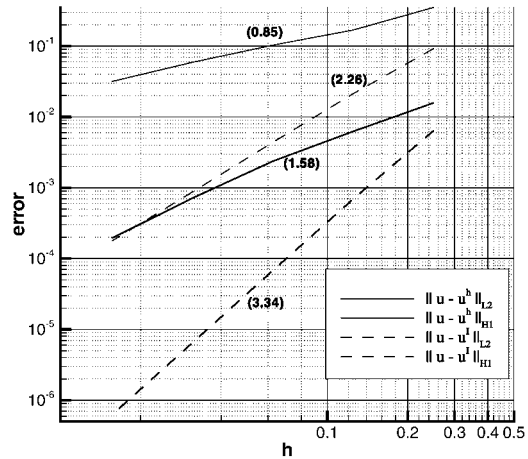


Figure 4. Error vs nodal spacing for 2D RKPM with boundary enrichment: results for  $p=2$ . Convergences rates are shown in parentheses.

The numerical solution is obtained on a regular square grid of RKPM nodes, separated by nodal spacing  $h$ . Once again, a support size of  $r=2.2h$  is used in computing the RKPM shape functions with a consistency of order  $p$ . Numerical integration is performed using 16 Gaussian quadrature points per integration cell.

Results are plotted in Figures 3 and 4 for  $p=1$  and 2, respectively. As predicted in Equations (21) and (22), the  $H1$  interpolation error is of order  $p$  while the  $L2$  interpolation error is of order  $p+1$ .

The solution errors show poor convergence rates for multiple dimensions, as predicted in Section 5. Comparing Figures 3 and 4 shows that these rates seem to be independent of  $p$ , and much less than the interpolation error convergence rates even for  $p=1$ . In Reference [6], Wagner and Liu trace this poor convergence to the inconsistency of the Galerkin weak form (34), which in turn results from the fact that  $V^h \not\subset V$  as alluded to in Section 5. An augmented weak form, which includes a boundary integral, was used in Reference [6] to correct this problem:

$$\int_{\Omega} \nabla v \cdot \nabla u \, d\Omega - \int_{\Gamma_g} v \mathbf{n} \cdot \nabla u \, d\Gamma = 0 \tag{35}$$

where in this case the essential boundary  $\Gamma_g$  is the entire boundary of  $\Omega$ . The convergence of the solution error using this augmented weak form for  $p=2$  is shown in Figure 5. For small  $h$ , the error is dependent on the number of quadrature points used for numerical integration; shown are results for both  $4 \times 4$  and  $6 \times 6$  Gaussian quadrature. As the number of integration points increases, the convergence rates approach the ideal values of  $p+1$  for  $L2$  error and  $p$  for  $H1$  error, demonstrating that integration error is the likely source of the slight deviation from the ideal convergence rates.

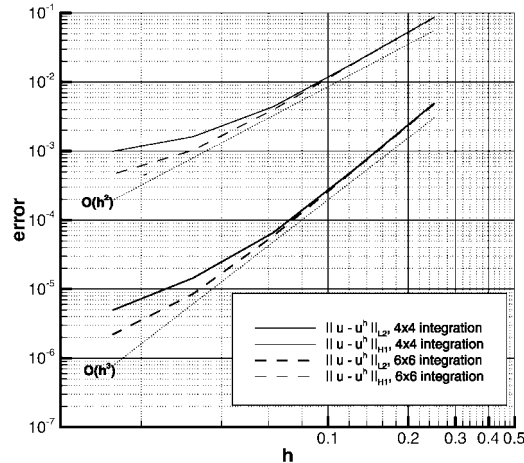


Figure 5. Error vs nodal spacing for 2D RKPM with boundary enrichment using augmented weak form (Equation (35)): results for  $p=2$ . Results approach the ideal convergence rates with increasing number of integration points.

#### REFERENCES

- Belytschko T, Lu YY, Gu L. Element-free Galerkin methods. *International Journal for Numerical Methods in Engineering* 1994; **37**:229–256.
- Krongauz Y, Belytschko T. Enforcement of essential boundary conditions in meshless approximations using finite elements. *Computer Methods in Applied Mechanics and Engineering* 1996; **131**:133–145.
- Chen JS, Wang HP. New boundary condition treatments in mesh-free computation of contact problems. *Computer Methods in Applied Mechanics and Engineering* 2000; **187**:441–468.
- Wagner GJ, Liu WK. Application of essential boundary conditions in mesh-free methods: a corrected collocation method. *International Journal for Numerical Methods in Engineering* 2000; **47**:1367–1379.
- Günther C, Liu WK. Implementation of boundary conditions for meshless methods. *Computer Methods in Applied Mechanics and Engineering* 1998; **163**:205–230.
- Wagner GJ, Liu WK. Hierarchical enrichment for bridging scales and mesh-free boundary conditions. *International Journal for Numerical Methods in Engineering* 2000; **50**:507–524.
- Liu WK, Uras RA, Chen Y. Enrichment of the finite element method with the reproducing kernel particle method. *Journal of Applied Mechanics, ASME* 1997; **64**:861–870.
- Belytschko T, Gu L, Lu YY. Fracture and crack growth by element-free Galerkin methods. *Modeling Simulations for Materials Science and Engineering* 1994; **2**:519–534.
- Liu WK, Jun S, Li S, Adee J, Belytschko T. Reproducing kernel particle methods for structural dynamics. *International Journal for Numerical Methods in Engineering* 1995; **38**:1655–1679.
- Liu WK, Jun S, Zhang YF. Reproducing kernel particle methods. *International Journal for Numerical Methods in Engineering* 1995; **20**:1081–1106.
- Duarte CA, Oden JT.  $H-p$  Clouds—an  $h-p$  meshless method. *Numerical Methods for Partial Differential Equations* 1996; **12**:673–705.
- Duarte CA, Oden JT. An  $h-p$  adaptive method using clouds. *Computer Methods in Applied Mechanics and Engineering* 1996; **139**:237–262.
- Babuška I, Melenk JM. The partition of unity finite element method. *International Journal for Numerical Methods in Engineering* 1997; **40**:727–758.
- Melenk JM, Babuška I. The partition of unity finite element method: basic theory and applications. *Computer Methods in Applied Mechanics and Engineering* 1996; **139**:289–314.
- Han W, Meng X. Error analysis of the reproducing kernel particle method. *Computer Methods in Applied Mechanics and Engineering*, to appear.
- Brenner SC, Scott LR. *The Mathematical Theory of Finite Element Methods*. Springer: New York, 1994.
- Ciarlet PG. *The Finite Element Method for Elliptic Problems*. North-Holland: Amsterdam, 1978.
- Liu WK, Shaofan Li, Belytschko T. Moving least-square reproducing kernel methods. Part I: methodology and convergence. *Computer Methods in Applied Mechanics and Engineering* 1997; **143**:113–154.